HHS Public Access

Author manuscript

Eur J Neurosci. Author manuscript; available in PMC 2015 April 13.

Published in final edited form as:

Eur J Neurosci. 2014 March ; 39(5): 757–770. doi:10.1111/ejn.12450.

Re-evaluation of connexins associated with motoneurons in rodent spinal cord, sexually dimorphic motor nuclei and trigeminal motor nucleus

W. Bautista[a], **J. E. Rash**[b], **K. G. Vanderpool**[b], **T. Yasumura**[b], and **J. I. Nagy**[a,*]

[a]Department of Physiology, Faculty of Medicine, University of Manitoba, Winnipeg, Canada

[b]Department of Biomedical Sciences, Colorado State University, Fort Collins, Colorado, USA

Abstract

Electrical synapses formed by neuronal gap junctions composed of connexin36 (Cx36) are a common feature in mammalian brain circuitry, but less is known about their deployment in spinal cord. It has been reported based on connexin mRNA and/or protein detection that developing and/or mature motoneurons express a variety of connexins, including Cx26, Cx32, Cx36 and Cx43 in trigeminal motoneurons, Cx36, Cx37, Cx40, Cx43 and Cx45 in spinal motoneurons, and Cx32 in sexually dimorphic motoneurons. We re-examined the localization of these connexins during postnatal development and in adult rat and mouse using immunofluorescence labelling for each connexin. We found Cx26 in association only with leptomeninges in the trigeminal motor nucleus, Cx32 only with oligodendrocytes and myelinated fibers among motoneurons in this nucleus and in the spinal cord, and Cx37, Cx40 and Cx45 only with blood vessels in ventral horn of spinal cord, including those among motoneurons. By freeze-fracture replica immunolabelling (FRIL, >100 astrocyte gap junctions but no neuronal gap junctions were found based on immunogold labeling for Cx43, whereas 16 neuronal gap junctions at P4, P7 and P18 were detected based on Cx36 labelling. Punctate labelling for Cx36 was localized to the somatic and dendritic surfaces of peripherin-positive motoneurons in the trigeminal motor nucleus, motoneurons throughout the spinal cord, and sexually dimorphic motoneurons at lower lumbar levels. In studies of electrical synapses and electrical transmission between developing and between adult motoneurons, our results serve to focus attention on mediation of this transmission by gap junctions composed of Cx36.

Keywords

Gap junctions; electrical coupling; sexually dimorphic motoneurons

Introduction

Gap junction channels between cells are composed of connexin proteins that form two apposed hexameric connexons linking across the extracellular space to allow the

[*]*Address for correspondence:* James I. Nagy, Department of Physiology, Faculty of Medicine, University of Manitoba, 745 Bannatyne Ave, Winnipeg, Manitoba, Canada R3E 0J9, nagyji@ms.umanitoba.ca, Tel. (204) 789-3767, Fax (204) 789-3934.

intercellular movement of ions and small molecules (Evans & Martin, 2002). Among the twenty connexin protein family members, most cells selectively express a particular connexin, although it is not unusual to find some cells concurrently producing two or even three different connexins (Yeh *et al*., 1998). The greatest diversity in the connexin composition of gap junctions is found in the central nervous system (CNS), perhaps not surprisingly given the cellular and morphological heterogeneity of neural tissue. With up to twelve different connexins found in adult brain, considerable efforts aimed to assign these to expression by particular cell types have lead to the consensus that astrocytes express Cx26, Cx30, and Cx43, and oligodendrocytes express Cx29, Cx32 and Cx47 (Rash *et al*., 2001a,b; Nagy *et al.*, 2004, 2011; Rash, 2010; Giaume, & Theis, 2010). In addition, a wide variety of neurons express Cx36 (Sohl *et al*., 2005; Meier & Dermietzel, 2006), while Cx45 and Cx57 exhibit more restricted neuronal expression, such as in retina (Hombach *et al*., 2004; Sohl *et al.*, 2005; Ciolofan *et al*., 2007; Li et al. 2008). Reporter gene expression of Cx30.2 has also been found in neurons (Kreuzberg *et al*., 2008), but corresponding expression of Cx30.2 protein has so far not been reported. Connexins in CNS vasculature have not been subject to comprehensive examination, but as in other tissues (Vis et al., 1998; Severs *et al.*, 2001), there is evidence in brain for Cx37 and Cx40 expression in endothelial cells, and Cx45 in vascular smooth muscle cells (Yeh *et al.*, 1998; Kruger et al., 2000; Li and Simard, 2001; Nagasawa *et al*., 2006; Haddock *et al.*, 2006).

The identification of cell-specific expression of connexins in brain has been essential for understanding the contribution of gap junctional intercellular communication to myriad of brain functions. In particular, the well established principle that gap junctions between neurons are the structural basis for electrical synaptic transmission (Bennett, 1997), together with the discovery of Cx36 expression in mammalian neurons (Condorelli *et al*., 1998; Sohl *et al*., 1998) and documentation of its widespread occurrence in neuronal gap junctions (Nagy *et al*., 2004; Sohl et al., 2005; Rash *et al*., 2000,2001a,b,2007a,b), provided the basis for numerous studies, leading to the general acceptance of the physiological importance of electrical synapses composed of Cx36 in mammalian brain (Bennett &, Zukin, 2004; Connors & Long, 2004; Hormuzdi *et al*., 2004).

In spinal cord, the organization of electrical synapses within neural circuitry, the functional roles of these synapses, the distribution of neuronal gap junctions, and the connexins that mediate electrical synaptic transmission are far less understood. As elsewhere in developing CNS, distinct populations of neurons in spinal cord are electrically coupled during development (Hinckley & Ziskind-Conhaim, 2006; Wilson *et al*., 2007), the most frequently cited example of which is coupling between motoneurons during roughly the first postnatal week, with reported subsequent loss of this coupling (Arasaki *et al*., 1984; Fulton *et al*., 1980; Walton & Navarette, 1991; Bou-Flores & Berger, 2001). In rodents, postnatal spinal motoneurons were reported to express five connexins, including Cx36, Cx37, Cx40, Cx43 and Cx45, with persistence of expression of Cx36, Cx37 and Cx40 in adult motoneurons (Chang *et al*., 1999; Chang & Balice-Gordon, 2000). It has also been reported that most spinal motoneurons express Cx32 (Micevych & Abelson, 1991), including motoneurons in sexually dimorphic motor nuclei (Matsumoto *et al*., 1991,1992), and that trigeminal motoneurons express Cx26, Cx32, Cx36, and Cx43 (Honma *et al.*, 2004), making the

claimed expression of seven connexins in a single cell type highly unusual. We have begun to focus our studies of electrical synapses on detailed examination of those associated with motoneurons, which could represent a daunting task given the plethora of connexins reported to be present in these cells. At the onset, therefore, we conducted a re-evaluation of expression of connexin proteins in motoneurons. We used immunofluorescence approaches to examine the localization of Cx32, Cx36, Cx37, Cx40, Cx43 and Cx45 in relation to rat and mouse spinal motoneurons, freeze-fracture replica immunogold labeling (FRIL) to assess Cx43 *vs* Cx36 protein in neurons *vs.* glia in rat lumbosacral spinal cord, and immunofluorescence of Cx26, Cx32, Cx36 and Cx43 in relation to trigeminal motoneurons in rats and mice.

Materials and methods

Animals and antibodies

The present immunofluorescence investigations were conducted using brains and spinal cords from fifteen adult C57BL/6 mice, two C57BL/6 Cx36 knockout mice, twenty adult Sprague-Dawley rats, and twelve mice and rats at various early postnatal ages. Colonies of C57BL/6-129SvEv wild-type and Cx36 knockout mice (Deans *et al*., 2001) were established at the University of Manitoba through generous provision of breeding pairs of these mice from Dr. David Paul (Harvard). Tissues from some of these animals were taken for use in parallel unrelated studies. Animals were utilized according to approved protocols by the Central Animal Care Committee of University of Manitoba and Colorado State University, with minimization of the numbers animals used.

All anti-connexin antibodies were obtained from Life Technologies Corporation (Grand Island, NY, USA) (formerly Invitrogen/Zymed Laboratories), and those used included: two rabbit polyclonal antibodies (Cat. No. 36-4600 and Cat. No. 51-6300) and one mouse monoclonal antibody (Cat. No. 39-4200) against Cx36; and rabbit polyclonal (Cat. No. 51-2800) and mouse monoclonal (Cat. No. 33-5800) antibodies Cx26, rabbit polyclonal antibodies against Cx32 (Cat. No. 34-5700), Cx37 (Cat. No. 42-4500), Cx40 (Cat. No. 36-5000 and Cat. No. 37-8900), Cx43 (Cat. No. 35-5000), and Cx45 (Cat. No. 40-7000). Specificity characteristics of the anti-Cx36 for Cx36 detection in various regions of rodent brain have been previously reported (Li *et al*., 2004; Rash et al., 2007a,b; Curti *et al*., 2012). Specificities of the anti-Cx26 and anti-Cx32, with confirmation using Cx26 ko and Cx32 ko mice, and that of anti-Cx43 have also been reported (Rash et al., 2001a; Nagy *et al*., 2003a, 2011). As described in the Results section, specificities of the anti-Cx37, anti-Cx40 and anti-Cx45 antibodies used are indicated by their labelling of each of their target connexins along blood vessels and, in the case of Cx40, labelling of gap junctions in heart, where each of these connexins are known to be expressed. In addition, the specificity of Cx37 and Cx40 detection by anti-Cx37 and anti-Cx40 along vasculature has been confirmed using Cx37 knockout and Cx40 knockout mice (A. Simon and JI Nagy, unpublished observations). Additional antibodies included a chicken polyclonal anti-peripherin that was utilized as a marker of motoneurons (Clarke et al., 2010) (Millipore, Temecula, CA, USA) and used at a dilution of 1:500, and a mouse monoclonal anti-2,’3’-cyclic nucleotide 3’-phosphodiesterase (CNPase) (Sternberger Monoclonals, Baltimore, MD, USA) that was utilized as a marker for

oligodendrocytes (Sprinkle, 1989) and used at a dilution of 1:1000. Various secondary antibodies included Cy3-conjugated goat or donkey anti-mouse and anti-rabbit IgG diluted 1:600 (Jackson ImmunoResearch Laboratories, West Grove, PA, USA), Alexa Flour 488-conjugated goat or donkey anti-rabbit and anti-mouse IgG diluted 1:600 (Molecular Probes, Eugene, OR, USA), AlexaFluor-647 conjugated goat anti-chicken IgG diluted 1:500 (Life Technologies Corporation) and Cy3-conjugated goat anti-chicken, diluted 1:600 (Jackson ImmunoResearch Laboratories). As a marker for blood vessels, we used AlexaFluor 647-conjucated isolectin B4 (IB4) (Invitrogen). All antibodies and IB4 were diluted in 50 mM Tris-HCl, pH 7.4, containing 1.5% sodium chloride (TBS), 0.3% Triton X-100 (TBSTr) and 10% normal goat or normal donkey serum.

Tissue preparation

Adult animals were deeply anesthetized with equithesin (3 ml/kg), placed on a bed of ice, and perfused transcardially with cold (4°C) pre-fixative consisting of 50 mM sodium phosphate buffer, pH 7.4, 0.1% sodium nitrite, 0.9% NaCl and 1 unit/ml of heparin, followed by perfusion with fixative solution containing cold 0.16 M sodium phosphate buffer, pH 7.4, 0.2% picric acid and either 1% or 2% formaldehyde prepared from freshly depolymerized paraformaldehyde. Animals were then perfused with a cold solution containing 10% sucrose and 25 mM sodium phosphate buffer, pH 7.4, to wash out excess fixative. Tissues from early postnatal animals were dissected and taken for immersion fixation in 1% or 2% formaldehyde for 30 to 50 min. Tissues were stored at 4°C for 24–48 h in cryoprotectant containing 25 mM sodium phosphate buffer, pH 7.4, 10% sucrose, 0.04% sodium azide. Sections of spinal cord were cut at a thickness of 10–15 μm using a cryostat and collected on gelatinized glass slides. Slide-mounted sections could be routinely stored at −35 °C for several months before use. Some detailed considerations regarding fixation conditions required for optimum immunohistochemical detection of Cx36, alone or in combination with other proteins, are described elsewhere (Nagy *et al*., 2012).

For FRIL, we prepared tissue and obtained relevant data from five postnatal rats – one at P4, two at P7, and two at P18. Rats were anesthetized using ketamine/xylazine, and prepared for electron microscopy by transcardiac perfusion with 2% or 4% formaldehyde in Sorenson's phosphate buffer, infiltrated with 30% glycerol, and freeze-fracture replicated in a JEOL JFD-2 or an RMC RFD 9000, according to our published procedures (Kamasawa *et al*., 2006). A total of 13 FRIL replicas were prepared and examined.

Immunofluorescence procedures

Slide-mounted sections removed from storage were air dried for 10 min, washed for 20 min in TBSTr, and processed for immunofluorescence staining, as described (Li et al., 2008; Bautista et al., 2012; Curti et al., 2012). For single-, double-, or triple-immunolabelling, sections were incubated with a single primary antibody, or simultaneously with two or three primary antibodies for 24 h at 4°C. All connexin antibodies were incubated with tissue sections at a concentration of 1–2 μg/ml. The sections were then washed for 1 h in TBSTr and incubated for 1.5 h at room temperature with either a single or appropriate combinations of secondary antibodies. Some sections processed by single or double immunolabelling were counterstained with either green Nissl fluorescent NeuroTrace (stain N21480) or Blue Nissl

NeuroTrace (stain N21479) (Molecular Probes, Eugene, OR, USA). All sections were coverslipped with the antifade medium Fluoromount-G (SouthernBiotech, Birmingham, AB, USA). Control procedures involving omission of one of the primary antibodies with inclusion of the secondary antibodies used for double- and triple-labelling indicated absence of inappropriate cross-reactions between primary and secondary antibodies for all of the combinations used in this study.

Immunofluorescence was examined on a Zeiss Axioskop2 fluorescence microscope and a Zeiss 710 laser scanning confocal microscope, using Axiovision 3.0 software or Zeiss ZEN Black 2010 image capture and analysis software (Carl Zeiss Canada, Toronto, Ontario, Canada). Data from wide-field and confocal microscopes were collected either as single scan images or z-stack images with multiple optical scans at z scanning intervals of typically 0.4 to 0.6 μm. Images of immunolabelling obtained with Cy5 fluorochrome were pseudo colored blue. Final images were assembled using CorelDraw Graphics (Corel Corp., Ottawa, Canada) and Adobe Photoshop CS software (Adobe Systems, San Jose, CA, USA).

For FRIL, we used antibodies against Cx36 (monoclonal 37–4600, polyclonal 51–6300 and 36–4600 from Life Technologies Corporation, and polyclonal Ab298 (Rash et al., 2000), and against Cx43 (MAB3068 from Millipore or 13–8300 from Life Technologies Corporation). Samples were counter labelled with various combinations of gold-conjugated secondary antibodies from BBI (5, 10, 20 and 30nm) and/or Jackson ImmunoResearch Laboratories Inc. (6-, 12- and 18-nm).

For transmission electron microscope (TEM) studies, samples were photographed as stereoscopic pairs with an 8° included angle using a JEOL 2000EX-II TEM or a JEOL JEM 1400 TEM equipped with a Gatan Orius SC1000 11 Megapixel digital camera. TEM negatives from the JEOL 2000 were scanned using an ArtixScan 2500f digital scanning device (Microtek) and processed using Photoshop CS2 (Adobe Systems). The contrast range for each image was optimized using “levels.” Slight image compressions created by photography of samples tilted for stereoscopy were corrected by using the “image distort” functions and trimmed so that the “stereo windows” appear rectangular and level.

Results

Connexins and spinal cord motoneurons

With the reported expression of seven connexin proteins and/or their corresponding mRNAs in motoneurons, we began by re-examining the distribution of immunofluorescence labelling for those connexins in lamina IX of spinal cord, and specifically their purported association with motoneurons. We first show that the antibodies used here against the relevant connexins produce immunolabelling patterns typical of those connexins localized to specific cell types. Anti-Cx37 and anti-Cx40 gave labelling along blood vessels in rat heart, as well as in rat and mouse brain (Fig. 1A–C), indicative of the localization of the connexins detected at gap junctions between endothelial cells (Severs *et al*., 2001). In addition, the anti-Cx40 gave labelling at intercalated discs and along lateral appositions of atrial cardiac myocytes in heart (Fig.1D and 1E), where Cx40-containing gap junctions are known to be heavily concentrated (Severs *et al*., 2001). The anti-Cx45 produced punctate labelling along

large diameter blood vessels in brain (Fig. 1F), reflective of Cx45 localization at gap junctions between smooth muscle cells along vasculature (Kruger *et al*., 2000; Li & Simard, 2001). Further, we have shown elsewhere that the anti-Cx45 used here labels ultrastructurally-identified inter-neuronal gap junctions in rodent retina (Li *et al*., 2008). Specificity validation of the other anti-connexin antibodies used is described in Materials and Methods. Confirmation that Cx37 and Cx40 are also localized along blood vessels in spinal cord is presented in Figures 1G and 1H. In the ventral horn of rat lumbar spinal cord, blood vessels labelled with the endothelial cell marker IB4 (Fig. 1G1 and H1) displayed similar labelling for Cx37 (Fig. 1G2) and Cx40 (Fig. 1G2) as seen along vessels in the cerebral cortex.

For studies of spinal cord, animals were examined at early developmental ages when spinal motoneurons were reported to express mRNA and/or protein for Cx36, Cx37, Cx40, Cx43, and Cx45, and at an adult stage when these neurons were found to continue expression of protein and/or mRNA for some of these same connexins (Chang et al., 1999; 2000; Chang & Balice-Gordon, 2000), as well as mRNA for Cx32 (Micevych & Abelson, 1991; Matsumoto *et al*., 1991,1992). We previously noted that labelling for Cx36 is present at sites between motoneurons at postnatal day (PD) 5 (Bautista *et al*., 2012). Here, we show that some motor nuclei display particularly robust immunolabelling for Cx36 at this age, as shown by examples with double labelling for Cx36 and the motoneuron marker peripherin (Clarke *et al.*, 2010) in lumbar spinal cord lamina IX of mouse (Fig. 2A,B) and rat (Fig. 2C). Labelling for Cx36 was exclusively punctate (Cx36-puncta), with absence of diffuse or punctate intracellular immunofluorescence. Although scattered sparsely in surrounding regions, Cx36-puncta were most concentrated within motor nuclei, were often localized to peripherin-positive motoneuronal somata or dendrites, and were commonly found at appositions between these neuronal elements (Fig. 2B,C). All clusters of motoneurons encountered displayed scattered Cx36-puncta, but there was considerable heterogeneity in density of Cx36-puncta among motor nuclei, suggesting staggered development of Cx36 expression among these nuclei.

For labelling of the various other connexins examined in fields of spinal cord lamina IX, results are presented with comparison of labelling for Cx36 in the same fields. All sections were triple labelled for Cx36 plus another connexin, with the inclusion of labelling for peripherin to ensure that areas examined contained groups of motoneurons; but labelling for peripherin is not always shown in order to avoid obscuring fine punctate labelling for connexins. In lumbar spinal cord sections labelled for Cx36 and Cx37, areas of lamina IX displaying Cx36-puncta showed immunofluorescence for Cx37 restricted to blood vessels in mouse at PD5 (Fig. 2D) and PD10 (Fig. 2E), and in rat at PD5 (Fig. 2F). [Labelling of all vascular-associated connexins (i.e., Cx37, Cx40 and Cx45) in spinal cord was sparse at these developmental ages, but where possible, was included in the fields photographed as positive controls for detection of these connexins with the antibodies used.] Similar result were obtained in comparisons of Cx36 and Cx37 expression in adult spinal cord. A low magnification of the ventral horn labelled for peripherin and counterstained with blue Nissl fluorescence is shown in Figure 2G, with the lower and upper boxed areas in this figure magnified in Figures 2H and 2I, respectively, which show labelling for Cx36, Cx37 and

peripherin. As seen at earlier ages, Cx36-puncta are distributed on peripherin-positive motoneurons in lamina IX (Fig. 2H), while labelling for Cx37 is absent on these motoneurons, but is instead seen localized along blood vessels, as shown by an example of a vessel in lamina VIII (Fig. 2I).

Double immunofluorescence labelling for peripherin and Cx43 in lamina IX of rat lumbar spinal cord at PD5 is shown in Fig. 2J. Labelling for Cx43 is entirely punctate, with negligible diffuse intracellular labelling, which was equal to background fluorescence seen after Cx43 primary antibody omission (not shown). In regions surrounding peripherin-positive motoneurons, Cx43-puncta are sparsely distributed at this age, and are not nearly as dense as seen throughout spinal cord gray matter in adults (Ochalski *et al*., 1997). Although resolution by immunofluorescence visualization is insufficient to discern whether or not some Cx43-puncta are localized directly on neuronal plasma membranes, these puncta did not display the regularity of association with peripherin-positive motoneuron dendrites and somata at PD5 as that displayed by Cx36-puncta. Adult motoneurons were also devoid of intracellular labelling for Cx43, but very densely distributed Cx43-puncta throughout neuropil precluded cell-type assignment of these puncta (not shown). In any case, Cx43 in adult spinal cord has been previously localized ultrastructurally to gap junctions between astrocytes, and not to those between neurons (Rash *et al*., 2001a; Ochalski *et al.*, 1997).

Labelling for Cx36 in combination with Cx45 in lamina IX of rat lumbar spinal cord at PD5 is shown in Figure 2K. Areas containing Cx36-puncta (Fig. 2K1) among motoneurons (peripherin labelling not shown) were totally devoid of labelling for Cx45 (Fig. 2K2). Labelling of Cx45 along blood vessels was encountered, but Cx45-puncta on these vessels were particularly sparse and fine at this age (not shown). In lamina IX of adult rat spinal cord, Cx36-puncta are seen decorating the surface of motoneurons (Fig. 2L1), but there is negligible association of labelling for Cx45 with those motoneurons. Instead Cx45-puncta displayed circular or elongated patterns of labelling (Fig. 2L1), as is more evident in the same field shown with labelling of Cx45 alone (Fig. 2L2), reflecting Cx45 localization at blood vessels cut perpendicular or tangential to their long axis.

Results from double labelling of Cx36 with Cx40, and peripherin with Cx40, in lumbar spinal cord are shown in Figure 3, where pairs of images (*e.g.*, A1,A2, etc) show Cx36 and Cx40 labelling, or peripherin and Cx40 labelling in the same field. As in the case of Cx37, fields containing Cx36-puncta in lamina IX at PD5 in rat (Fig. 3A1) and mouse (Fig. 3B1), and at PD10 in mouse (Fig. 3C1), showed an absence of labelling for Cx40 associated with motoneurons (labelling for peripherin not shown), but did display labelling of Cx40 along with blood vessels in the same fields (Fig. 3A2, 3B2, and 3C2). Examples of labelling for peripherin in conjunction with Cx40 in lumbar lamina IX at PD5 are shown in rat (Fig. 3D) and mouse (Fig. 3E), where areas filled with peripherin-positive motoneurons (Fig. 3D1 and 3E1) displayed labelling for Cx40 restricted exclusively to blood vessels in the vicinity of these neurons (Fig. 3D2 and 3E2, respectively). Similar results were obtained in adult cord, where peripherin-positive motoneurons in lamina IX (Fig. 3F1) showed an absence of labelling for Cx40, and Cx40 was localized instead to blood vessels (Fig. 3F2).

FRIL localization of Cx36 and Cx43 in developing spinal cord

Given the limitations discussed above in assigning cell-type localization of Cx43 by immunofluorescence, labelling for Cx43 vs Cx36 in developing spinal cord was examined by FRIL (Fig. 4). For FRIL, both single-labelling for Cx43 or Cx36 (sometimes with additional labeling for other connexins, such as Cx32 and Cx26), and double-labeling for Cx43 plus Cx36 revealed labelling for Cx43 only in astrocyte, ependymocyte, and leptomeningeal gap junctions (Fig. 4B), and Cx36 only in neuronal gap junctions (Fig. 4A), and in double-labeled samples, with Cx43 found in nearby astrocyte gap junctions. Specifically, we found Cx43 only in glial and leptomeningeal gap junctions at P4 (two replicas, 15 GJs Fig. 4B), P7 with four replicas all double-labelled for Cx36 and Cx43, revealing 5 neuronal GJs labelled for Cx36 without Cx43 (Fig. 4A), and 18 astrocyte GJs labelled for Cx43 but not Cx36, and P18 with eight replicas, including one double labelled for Cx43 plus Cx36, which revealed >100 A/A and O/A gap junctions containing only Cx43 and eleven neuronal gap junctions containing only Cx36.

Localization of Cx36 and Cx32 among sexually dimorphic motor nuclei

Sexually dimorphic motor nuclei, together with their constituent motoneurons, are defined as such because the morphological appearance and numbers of neurons in these nuclei differ substantially in male and female species (Breedlove, 1986; McKenna & Nadelhaft 1986; Coleman & Sengelaub, 2002). Located at the lumbosacral L6–S1 levels, these nuclei consist of several groups, including a dorsomedial group and a dorsolateral group, on which we fous here. A more comprehensive analysis of Cx36 association with these nuclei is given elsewhere (Bautista *et al*., 2013a).

Comparison of Cx36 with Cx32 localization in spinal cord was examined in sexually dimorphic motor nuclei in which motoneurons were reported to express Cx32 mRNA (Matsumoto *et al*., 1991,1992), and well as in other motor nuclei where in situ hybridization signal for Cx32 mRNA was detected, although we appreciate caveats noted regarding specificity of Cx32 mRNA detection (Micevych & Abelson, 1991). Immunofluorescence labelling for Cx36 and Cx32 among peripherin-positive motoneurons in lamina IX of adult male rats is shown in Figure 5. At lower lumbar spinal levels, containing the locations of sexually dimorphic nuclei (McKenna & Nadelhaft, 1986), labelling for Cx36 was detected in each of these nuclei, as shown by examples of Cx36 localization in the dorsomedial nucleus at its rostral (Fig. 5A) and caudal (Fig. 5B) levels, and in the dorsolateral nucleus at a rostral level (Fig. 5C). At higher magnification, Cx36-puncta were readily seen associated with the somata and dendrites of peripherin-positive dimorphic motoneurons, as shown in the dorsomedial nucleus (Fig. 5D). In contrast, labelling for Cx32 was sparse in the dimorphic motor nuclei, and was absent on the surface of, or intracellularly within, these motoneurons, but was instead localized to small cells that were delineated by Cx32-puncta decorating their surface (Fig. 5A–D) or was associated with strands of fibers, which resembled patterns of labelling we have previously reported for Cx32 associated with oligodendrocytes and myelinated fibers (Nagy *et al*., 2003a,b). Examination of other spinal levels containing non-dimorphic motor nuclei in lamina IX showed a similar association of Cx36 with peripherin-positive motoneurons and an absence of Cx32 localization at the surface of these neurons (Fig. 5E). In adult male mice, the sexually dimorphic Onuf’s motor

nucleus located at the L6 spinal level, and corresponding roughly to the dorsomedial and dorsolateral nuclei in rat, also displayed Cx36-puncta associated with motoneurons (Fig. 5F1), whereas Cx32 was again localized to small cells (Fig. 5F2) that had the size and shape of oligodendrocytes. As in rat, similar results were obtained in non-dimorphic motor nuclei of mouse at other spinal levels, where motoneurons displayed labelling for Cx36 but not Cx32 along their somatic and dendritic surfaces (Fig. 5G). Confirmation of Cx32 localization to oligodendrocytes was obtained by triple labelling for Cx32, peripherin and the oligodendrocyte marker CNPase (Fig. 5H,I), revealing Cx32-puncta distributed on the surface of CNPase-positive cells in lamina IX of lumbar spinal cord. Additional Cx32-puncta not associated with oligodendrocyte somata or with motoneurons were localized along myelinated fibers, as we have previously shown in regions elsewhere in the CNS (Nagy *et al.*, 2003a,b).

Connexins and trigeminal motoneurons

We next examined immunofluorescence localization of Cx26, Cx32, Cx36 and Cx43 in the trigeminal motor nucleus of PD15 and adult mouse, where diffuse labelling for each of these connexins was described to occur in the cytoplasm and/or nucleus of trigeminal motor neurons of developing and adult mice (Honma et al., 2004). In adult mice, labelling of Cx36 was distributed throughout the trigeminal motor nucleus, and was remarkably dense to the point of delineating the nucleus from surrounding regions that contained sparse labelling (Fig. 6A). Immunofluorescence consisted exclusively of Cx36-puncta often localized to the surface of peripherin-positive motoneuron somata or along their dendrites (Fig. 6B). Punctate or diffuse intracellular labelling is absent, as determined by through focus confocal analysis of individual motoneurons and by comparison of intracellular labelling in motoneurons with background fluorescence in these neurons after omission of primary antibody. Specificity of Cx36 detection in the trigeminal motor nucleus by the antibodies used is shown by absence of immunolabelling with these antibodies in Cx36 knockout mice, as indicated in supplementary Figure S1, showing a similar field of the nucleus in the knockout mice as shown in Figure 6A of wild-type mice.

Comparison of labelling for Cx36 and Cx26 among adult trigeminal motoneurons is shown in Figure 6C. In contrast to widely distributed Cx36-puncta (Fig. 6C1), labelling for Cx26 is restricted to a lateral portion of the nucleus largely devoid of motoneuron somata, but containing myelinated fibers belonging to the motor root of the trigeminal nerve (Fig. 6C2). Immunofluorescence for Cx26 is punctate in appearance, and displayed negligible association with trigeminal motoneuronal somata. Diffuse intracellular labelling for Cx26 in these somata is also negligible. Elsewhere in brain, similar parenchymal Cx26-puncta in adult rodent were localized to astrocyte processes labelled for glial fibrillary acidic protein (GFAP) (Nagy et al., 2001, 2011). The trigeminal motor nucleus and the motor root of the trigeminal nerve laying lateral to it were largely devoid of labelling for GFAP under the fixation conditions required to detect Cx26, precluding double labelling for this connexin and the astrocyte marker. At PD15, localization of Cx36 among trigeminal motoneurons was somewhat less dense, and consisted of finer Cx36-puncta (Fig. 6D) than seen in adult mice, suggesting that Cx36-puncta increase in size and density with development, notwithstanding that earlier postnatal ages were not examined. This is in contrast to the reduced labelling for

Cx36 previously reported in these motoneurons during development (Honma *et al.*, 2004). Labelling for Cx26 in the trigeminal motor nucleus was absent at PD15, except for Cx26 seen in association with leptomeningeal sheaths of blood vessels, where these meningeal sheath have short projections into the brain (Mercier & Hatton, 2001).

Immunofluorescence labelling for Cx32 in combination with that of either Cx36 and peripherin or with the oligodendrocytes marker CNPase and peripherin in the trigeminal motor nucleus in adult mouse is shown in Figure 6E–G. Labelling of Cx32 was punctate, similar to that of Cx36, but was often assembled in round or oval clusters (Fig. 5E,F), and was absent intracellularly in motoneurons. Again, in contrast to the regular localization of Cx36 to the surface of peripherin-positive motoneurons (Fig. 6E,F), Cx32-puncta usually appeared in areas devoid of labelling for peripherin. Where overlap between these puncta and peripherin occurred in z-stack images, 3-dimensional rotation indicated lack of association of puncta with motoneuron surfaces (not shown). Inclusion of labelling for CNPase revealed the clusters of Cx32-puncta to be associated with CNPase-positive oligodendrocytes and their initial dendritic segments (Fig. 6G). Some CNPase signal (red) was seen above or below (confirmed in single scans) peripherin signal (blue) in these 5 μm z-stack images, but stacks were required to obtain a full complement of Cx32-puncta around oligodendrocytes. Similar labelling and localization of Cx32 to oligodendrocytes was seen in mouse trigeminal motor nucleus at PD15 (not shown).

Triple immunofluorescence labelling for Cx36, Cx43 and peripherin in the trigeminal motor nucleus of adult mouse is shown in Figure 6H and I, with similar patterns of labelling observed in this nucleus at PD15 (not shown). Labelling for Cx43 was punctate throughout the brainstem, including the trigeminal motor nucleus, and Cx43-puncta were exceptionally dense compared with that of Cx36-puncta (Fig. 6H). Although Cx43-puncta were observed lying over peripherin-positive motoneuron dendrites in the z-stack image shown in Fig. 6I, and Cx36-puncta were seen lying over these neurons in Figure 6G3, 6F and 6I, through focus analysis indicated absence of intracellular punctate or diffuse Cx43 or Cx36 immunoreactivity. Regardless of whether images were captured as confocal z-stack or as single scans, some Cx43-puncta were invariably found to lie very near peripherin-positive elements, making it impossible by immunofluorescence light microscopy to assign these puncta to plasma membranes of particular cell types. Nevertheless, given the localization of Cx43 to astrocyte gap junctions in most other brain regions, together with the close proximity of some of these junctions to the plasma membranes of neuronal somata and dendritic (Yamamoto *et al.*, 1990), which can be <0.5 μm, the close proximity of some Cx43-puncta to trigeminal motoneuron somata and their processes is expected assuming localization of these puncta to astrocyte gap junctions, as was confirmed by FRIL in all other areas of the CNS that we have examined (Nagy *et al.*, 2004; Rash & Yasumura, 1999; Rash *et al.*, 1998a,b, 2000, 2001a,b; 2007a,b), and supported by FRIL in the current study.

Discussion

Extensive gap junctional coupling between neurons throughout the CNS at early postnatal ages is a hallmark of developing neural systems (Meier & Dermietzel, 2006). It has more recently become well established that electrical synapses persist, at higher or lower levels

than seen during deveopment, in many CNS areas of adult animals, where they contribute essential features to integrative processes in neuronal circuitry (Bennett &, Zukin, 2004; Connors & Long, 2004; Hormuzdi *et al*., 2004; Rash et al., 2013). Despite earlier acceptance of widespread electrical synapses at early postnatal ages, less is currently known about the functional role of electrical coupling between neurons during development. This is particularly the case in the spinal cord, where detailed studies of neuronal gap junction localization and connexin expression patterns, both during development and at maturity, have lagged behind those in brain, making it difficult to relate presence of electrical coupling to incidence and distribution of the morphological substrate of this coupling, namely neuronal gap junctions. Some of the literature available on coupling between motoneurons is especially fraught with considerable complexity.

Electrical coupling between early postnatal motoneurons, suggested to be important for generation of synchronous activity among these neurons (Kiehn & Tresch, 2002; Kiehn et al., 2000), was found to be either reduced (Tresch & Kiehn, 2000) or to be unaffected (Tresch & Kiehn, 2002) by gap junction blockers. In a series of long-standing reports, motoneuron coupling was considered in the context of synapse development with target muscles in both intact and peripheral nerve-transected animals (Personius & Balice-Gordon, 2001). In these studies in rodents and cats, postnatal motoneurons were found apparently to express five connexins, including Cx36, Cx37, Cx40, Cx43 and Cx45, with persistence of expression of the former three connexins in adults, despite loss of coupling, and reported presence of motoneuron plasma membrane labeling for Cx43 protein (Chang *et al*., 1999; Chang & Balice-Gordon, 2000). Our finding regarding Cx45 are consistent with the reported absence of EGFP reporter expression for Cx45 in the spinal cord ventral horn of transgenic mice (Chapman *et al*., 2013). Further, motoneuron coupling was reduced in mice with Cx40 knockout, which had an impact on patterns of neuromuscular synapse development (Personius & Balice-Gordon, 2000; Personius *et al*., 2001,2007). Reports generally refer to a loss of motoneuronal gap junctional coupling during maturation. However, gap junctions were observed between some motoneurons in adult rodent spinal cord (van der Want *et al*., 1998), particularly between motoneurons in sexually dimorphic motor nuclei (Matsumoto *et al*., 1988,1989), which is consistent with the persistence of coupling among motoneuronal populations in the dimorphic nuclei of adult animals (Coleman & Sengelaub, 2002), and which was attributed to expression of Cx32 in these dimorphic motoneurons (Matsumoto *et al*., 1991,1992). In animals subjected to various treatments, there have been reports of altered motoneuronal coupling without changes (Chang *et al*., 2000) or undetermined changes (Mentis *et al*., 2002; Pastor *et al*., 2003) in connexin expression, or altered Cx36 expression in unidentified cell types without determination of possible changes in coupling (Yates *et al*., 2011). As in spinal cord, complex patterns of connexin expression have also been reported in the trigeminal motor nucleus, where largely diffuse cytoplasmic immunolabelling and even some nuclear immunolabelling for Cx26, Cx32 and Cx43 was described in both developing and adult trigeminal motoneurons (Honma *et al*., 2004).

In a previous report, we described a deficit in presynaptic inhibition in the spinal cord of juvenile mice with Cx36 knockout, correlated this with the presence of Cx36 and neuronal dye-coupling among interneurons that mediate presynaptic inhibition, and noted the

persistence of Cx36 expression in various dorsal and ventral horn regions in adult rodent spinal cord, including labelling of Cx36 in association with motoneurons (Bautista *et al*., 2012). The present analyses of various connexin proteins reported to be expressed in developing and adult rodent spinal cord reveals robust and consistent punctate labelling for Cx36 in motor nuclei, often localized to the surface of motoneurons in spinal cord lamina IX and the trigeminal motor nucleus, compared with the absence of similar labelling for the other connexin proteins examined. Localization of Cx37, Cx40 and Cx45 was restricted to blood vessels in this and other spinal cord laminae, and Cx43 showed little evidence of a regular association with motoneurons at early stages of development. Nor did we find Cx37 or Cx45 localized to spinal motoneurons or intracellular diffuse labelling or diffuse plasma membrane labelling of Cx43 protein in these neurons of adult animals, contrasting with earlier descriptions of multiple connexin in those cells (Chang *et al*., 1999; Chang & Balice-Gordon, 2000). Further, despite reports of widespread Cx32 mRNA expression in spinal motoneurons (Micevych & Abelson, 1991), including sexually dimorphic motoneurons (Matsumoto *et al*., 1991,1992), we found Cx32 protein to be associated only with oligodendrocytes and myelinated fibers in lamina IX, as well as in other spinal cord laminae. Similarly, in the trigeminal motor nucleus, we found Cx26 only in association with bundles of white matter and with leptomeninges, and Cx32 only with oligodendrocytes, as occurs elsewhere in brain (Nagy *et al.*, 2003; Lynn *et al.*, 2011), and no evidence of previously described diffuse cytoplasmic or nuclear labelling for these connexins (Honma *et al.*, 2004) or for that of Cx36 or Cx43 in trigeminal motoneurons. It should be noted that, due to limits of resolution afforded by immunofluorescence microscopy, very dense punctate labelling for Cx43 in all areas of the CNS precludes assignment of this labelling to plasma membranes of specific cell types, even though such correlations had been made previously (Chang et al., 1999, 2000; Honma *et al.*, 2004).

Our results stand in marked contrast to previous reports of Cx40, Cx43 and Cx45 protein expression in spinal motoneurons, and Cx26, Cx32 and Cx43 expression in trigeminal motoneurons. Further, our data cast doubt on connexin protein expression from mRNAs for some of these connexins and for mRNAs for Cx32 and Cx37 reported to be present in motoneurons (Matsumoto *et al*., 1991,1992; Micevych & Abelson, 1991; Chang *et al.*, 1999, 2000; Chang & Balice-Gordon, 2000; Honma *et al.*, 2004). It appears that these mRNAs in motoneurons are repressed by specific miRNAs (Smirnova et al., 2005) and are not translated into corresponding protein products, including neuron-specific vs. glial cell-specific connexins (Rash et al., 2005). Our results are consistent with ultrastructural localization of Cx32 and Cx43 to gap junctions between glial cells in the spinal cord, and not to those between neurons (Rash *et al*., 1998a,b; 2001a). Previously reported reductions in motoneuron coupling and disruptions in motoneuron synaptic organization in Cx40 knockout mice (Personius et al., 2007) may have arisen from vascular and/or cardiac anomalies in these animals (Simon & McWhorter, 2002), rather than to effects on neuronal gap junctions. We conclude that Cx36 is the major connexin mediating electrical and dye-coupling between rodent motoneurons at early postnatal ages and in sexually dimorphic motoneurons in adult animals, and suggest that Cx36 be the focus of continued studies of motoneuronal gap junctions in rodent spinal cord. Nevertheless, in absence of data indicating total loss of coupling between motoneurons during early development in Cx36

knockout mice, we cannot exclude the possibility that these neurons may express another as yet unidentified connexin, either normally or in a compensatory fashion in the Cx36 knockout, particularly since Cx36-expressing neurons in some systems were reported to display residual coupling after Cx36 ablation (Lee *et al*., 2010; Curti *et al*., 2012). It may be noted that any additional connexins expressed in motoneurons would appears to exclude Cx30.2, because reporter expression for Cx30.2 was not found in these neurons (Kreuzberg et al., 2008).

Cx36 association with adult motoneurons

The abundant Cx36-puncta associated with adult motoneurons in sexually dimorphic motor nuclei almost certainly reflect visualization of gap junctions, consistent with demonstrations of dye-coupling between these neurons in adult rats (Coleman & Sengelaub, 2002). However, relatively high densities of Cx36-puncta are also widely distributed on lamina IX motoneurons elsewhere and, indeed, throughout the spinal cord, as well as on motoneurons in the trigeminal motor nucleus in adult rodents. Because electrical- and dye-coupling between motoneurons is well-established to progressively decrease and perhaps to disappear during development (Walton & Navarette, 1991; Chang et al, 1999), it may be considered that Cx36-containing gap junctions associated with adult spinal motoneurons in other than sexually dimorphic motor nuclei are unable to support functional coupling, at least at spinal levels that have been studied (coupling of trigeminal motoneurons has not been examined in developing or adult animals). To reconcile lack of coupling between non-dimorphic adult motoneurons with the presence of Cx36-puncta on these neurons, it should be noted that we have found these puncta to be associated with axon terminals that contain vescicular glutamtate transporter1 (vglut1) and that are of primary afferent origin (Bautista *et al.*, 2013a,b), apparently forming the morphologically mixed synapses that have been described in ultrastructural studies of spinal cord (Rash et al., 1996). Such mixed synapses are potentially capable of chemical/electrical transmission, and their presynaptic fibers in other systems appear to be capable of supporting electrical coupling between neurons that receive these synapses, as is seen in rodent vestibular nuclei (see Nagy et al., 2013), and as has been suggested in the hippocampus (Nagy, 2012). Conditions under which a similar mechanism may endow mixed synapses with the ability to support coupling between spinal motoneurons remain to be determined.

Supplementary Material

Refer to Web version on PubMed Central for supplementary material.

Acknowledgements

This work was supported by a grant from the Canadian Institutes of Health Research to J.I.N. (MOP 106598) and to DM (MOP 37756), and by grants from the National Institutes of Health (NS31027, NS44010, NS44295 to JER. We thank B. McLean for excellent technical assistance, Dr. B. Lynn for genotyping of transgenic mice, Dr. D. Paul (Harvard University) for providing breeding pairs of Cx36 knockout and wild-type mice, and Dr. A. Simon (University of Arizona) for collaborations in testing specificity of anti-Cx37 and anti-Cx40 antibodies in Cx37 and Cx40 knockout mice.

Abbreviations

CNS	Central nervous system
CNPase	anti-2,’3’-cyclic nucleotide 3’-phosphodiesterase
Cx36	connexin36
L	lumbar
Mo5	trigeminal motor nucleus
PBS	phosphate-buffered saline
PD	postnatal day
TBS	50 mM Tris-HCl, pH 7.4, 1.5% NaCl
TBSTr	TBS containing 0.3% Triton X-100
vglut1	vescicular glutamtate transporter1

References

Arasaki K, Kudo N, Nakanishi T. Firing of spinal motoneurons due to electrical interactions in the rat: an in vitro study. Exp. Brain Res. 1984; 54:437–445. [PubMed: 6723863]

Bautista W, Nagy JI, Dai Y, McCrea DA. Requirement of neuronal connexin36 in pathways mediating presynaptic inhibition of primary afferents in functionally mature mouse spinal cord. J Physiol. 2012; 590:3821–3839. [PubMed: 22615430]

Bautista W, Nagy JI. Connexin36 in gap junctions forming electrical synapses between motoneurons in sexually dimorphic motor nuclei in spinal cord of rat and mouse. Neuroscience. 2013a In Press.

Bautista W, McCrea DA, Nagy JI. Connexin36 identified at primary afferent terminals forming morphologically mixed chemical/electrical synapses in adult rodent spinal cord. 2013b Submitted.

Bennett MVL. Gap junctions as electrical synapses. J. Neurocytol. 1997; 26:349–366. [PubMed: 9278865]

Bennett MVL, Zukin SR. Electrical coupling and neuronal synchronization in the mammalian brain. Neuron. 2004; 41:495–511. [PubMed: 14980200]

Bou-Flores C, Berger AJ. Gap junctions and inhibitory synapses modulate inspiratory motoneuron synchronization. J. Neurophysiol. 2001; 85:1543–1551. [PubMed: 11287478]

Breedlove SM. Cellular analysis of hormone influence on motoneuronal development and function. J. Neurobiol. 1986; 17:157–176. [PubMed: 3519862]

Chang Q, Balice-Gordon RJ. Gap junctional communication among developing and injured motor neurons. Brain Res. Rev. 2000; 3:242–249. [PubMed: 10751674]

Chang Q, Gonzalez M, Pinter MJ, Balice-Gordon RJ. Gap junctional coupling and patterns of connexin expression among neonatal rat lumbar spinal neurons. J. Neurosci. 1999; 19:10813–10828. [PubMed: 10594064]

Chang Q, Pereda A, Pinter MJ, Balice-Gordon RJ. Nerve injury induces gap junctional coupling among axotomized adult motor neurons. J. Neurosci. 2000; 20:674–684. [PubMed: 10632597]

Chapman RJ, Lall VK, Maxeiner S, Willecke K, Deuchars J, King AE. Localization of neurones expressing the gap junction protein connexin45 within the adult spinal dorsal horn: a study using Cx45-eGFP reporter mice. Brain Struct. Funct. 2013; 218:751–765. [PubMed: 22638825]

Ciolofan C, Lynn BD, Wellershaus K, Willecke K, Nagy JI. Spatial relationships of connexin36, connexin57 and zonula occludens-1 (ZO-1) in the outer plexiform layer of mouse retina. Neuroscience. 2007; 148:473–488. [PubMed: 17681699]

Clarke WT, Edwards B, McCullagh KJ, Kemp MW, Moorwood C, Sherman DL, Burgess M, Davies KE. Syncoilin modulates peripherin filament networks and is necessary for large-calibre motor neurons. J. Cell Sci. 2010; 123:2543–2552. [PubMed: 20587592]

Coleman AM, Sengelaub DR. Patterns of dye coupling in lumbar motor nuclei of the rat. J. Comp. Neurol. 2002; 454:34–41. [PubMed: 12410616]

Condorelli DF, Parenti R, Spinella F, Salinaro AT, Belluardo N, Cardile V, Cicirata F. Cloning of a new gap junction gene (Cx36) highly expressed in mammalian brain neurons. Eur. J. Neurosci. 1998; 10:1202–1208. [PubMed: 9753189]

Connors BW, Long MA. Electrical synapses in the mammalian brain. Annu. Rev. Neurosci. 2004; 27:393–418.

Curti S, Hoge G, Nagy JI, Pereda AE. Synergy between electrical coupling and membrane properties promotes strong synchronization of neurons of the mesencephalic trigeminal nucleus. J. Neurosci. 2012; 32:4341–4359. [PubMed: 22457486]

Deans MR, Gibson JR, Sellitto C, Connors BW, Paul DL. Synchronous activity of inhibitory networks in neocortex requires electrical synapses containing connexin36. Neuron. 2001; 31:477–485. [PubMed: 11516403]

Evans WH, Martin PEM. Gap junctions: structure and function. Mol. Membr. Biol. 2002; 19:121–136. [PubMed: 12126230]

Fulton BP, Miledi R, Takahashi T. Electrical synapses between motoneurons in the spinal cord of the newborn rat. Proc. R. Soc. London, Ser. B. 1980; 206:115–120. [PubMed: 6105652]

Giaume C, Theis M. Pharmacological and genetic approaches to study connexin-mediated channels in glial cells of the central nervous system. Brain Res. Rev. 2010; 63:160–176. [PubMed: 19963007]

Haddock RE, Grayson TH, Brackenbury TD, Meaney KR, Neylon CB, Sandow SL, Hill CE. Endothelial coordination of cerebral vasomotion via myoendothelial gap junctions containing connexins 37 and 40. Am. J. Physiol. Heart Circ. Physiol. 2006; 291:H2047–H2056. [PubMed: 16815985]

Hinckley CA, Ziskind-Conhaim L. Electrical coupling between locomotor-related excitatory interneurons in the mammalian spinal cord. J. Neurosci. 2006; 26:8477–8483. [PubMed: 16914672]

Hombach S, Janssen-Bienhold U, Sohl G, Schubert T, Bussow H, Ott T, Weiler R, Willecke K. Functional expression of connexin57 in horizontal cells of the mouse retina. Eur. J. Neurosci. 2004; 19:2633–2640. [PubMed: 15147297]

Honma S, De S, Li D, Shuler CF, Turman JE Jr. Developmental regulation of connexins 26, 32, 36 and 43 in trigeminal neurons. Synapse. 2004; 52:258–271. [PubMed: 15103692]

Hormuzdi SG, Filippov MA, Mitropoulon G, Monyer H, Bruzzone R. Electrical synapses: a dynamic signaling system that shapes the activity of neuronal networks. Biochem. Biophys. Acta. 2004; 1662:113–137. [PubMed: 15033583]

Kamasawa N, Furman CS, Davidson KGV, Sampson JA, Magnie AR, Gebhardt BR, Kamasawa M, Yasumura T, Zumbrunnen JR, Pickard GE, Nagy JI, Rash JE. Abundance and ultrastructural diversity of neuronal gap junctions in the OFF and ON sublaminae of the inner plexiform layer of rat and mouse retina. Neuroscience. 2006; 142:1093–1117. [PubMed: 17010526]

Kiehn O, Kjaerulff O, Tresch MC, Harris-Warrick RM. Contributions of intrinsic motor neuron properties to the production of rhythmic motor output in the mammalian spinal cord. Brain Res. Bull. 2000; 53:649–659. [PubMed: 11165800]

Kiehn O, Tresch MC. Gap junctions and motor behavior. Trends Neurosci. 2002; 25:108–115. [PubMed: 11814564]

Kreuzberg MM, Deuchars J, Weiss E, Schober A, Sonntag S, Wellershaus K, Draguhn A, Willecke K. Expression of connexin30.2 in interneurons of the central nervous system in the mouse. Mol. Cell Neurosci. 2008; 37:119–134. [PubMed: 17942321]

Kruger O, Plum A, Kim J-S, Winterhager E, Maxeiner S, Hallas G, Kirchhoff S, Traub O, Lamers WH, Willecke K. Defective vascular development in connexin45-deficient mice. Development. 2000; 127:4179–4193. [PubMed: 10976050]

Lee SC, Cruikshank SJ, Connors BW. Electrical and chemical synapses between relay neurons in developing thalamus. J. Physiol. 2010; 588:2403–2415. [PubMed: 20457735]

Li X, Olson C, Lu S, Kamasawa N, Yasumura T, Rash JE, Nagy JI. Neuronal connexin36 association with zonula occludens-1 protein (ZO-1) in mouse brain and interaction with the first PDZ domain of ZO-1. Eur. J. Neurosci. 2004; 19:2132–2146. [PubMed: 15090040]

Li X, Kamasawa N, Ciolofan C, Olson CO, Lu S, Davidson KGV, Yasumura T, Shigemoto R, Rash JE, Nagy JI. Connexin45-containing neuronal gap junctions in rodent retina also contain connexin36 in both apposing hemiplaques, forming bi-homotypic gap junctions, with scaffolding contributed by zonula occludens-1. J. Neurosci. 2008; 28:9769–9789. [PubMed: 18815262]

Li X, Simard JM. Connexin45 gap junction channels in rat cerebral vascular smooth muscle cells. Am. J. Physiol. 2001; 281:1890–1898.

Lynn BD, Tress O, May D, Willecke K, Nagy JI. Ablation of connexin30 in transgenic mice alters expression patterns of connexin26 and connexin32 in glial cells and leptomeninges. Eur. J. Neurosci. 2011; 11:1783–1793. [PubMed: 22098503]

Matsumoto A, Arnold AP, Micevych PE. Gap junctions between lateral spinal motoneurons in the rat. Brain Res. 1989; 495:362–366. [PubMed: 2765937]

Matsumoto A, Arnold AP, Zampighi G, Micevych PE. Androgenic regulation of gap junctions between motoneurons in the rat spinal cord. J. Neurosci. 1988; 8:4177–4183. [PubMed: 3183718]

Matsumoto A, Arai Y, Urano A, Hyodo S. Androgen regulates gap junction mRNA expression in androgen-sensitive motoneurons in the rat spinal cord. Neurosci. Let. 1991; 131:159–162. [PubMed: 1662339]

McKenna KE, Nadelhaft I. The organization of the pudendal nerve in the male and female rat. J. Comp. Neurol. 1986; 248:532–549. [PubMed: 3722467]

Matsumoto A, Arai Y, Urano A, Hyodo S. Effect of androgen on the expresssion of gap junction and beta-actin mRNAs in adult rat motoneurons. Neurosci. Res. 1992; 14:133–144. [PubMed: 1326732]

Meier C, Dermietzel R. Electrical synapses--gap junctions in the brain. Results Probl. Cell Differ. 2006; 43:99–128. [PubMed: 17068969]

Mercier F, Hatton GI. Connexin26 and basic fibroblast growth factor are expressed primarily in the subpial and subependymal layers in adult brain parenchyma: roles in stem cell proliferation and morphological plasticity? J. Comp. Neurol. 2004; 431:88–104. [PubMed: 11169992]

Mentis GZ, Diaz E, Moran LB, Navarrete R. Increased incidence of gap junctional coupling between spinal motoneurons following transient blockade of NMDA receptors in neonatal rats. J Physiol. 2002; 544:757–764. [PubMed: 12411521]

Micevych PE, Abelson L. Distribution of mRNAs coding for liver and heart gap junction proteins in the rat central nervous system. J. Comp. Neurol. 1991; 305:96–118. [PubMed: 1851768]

Nagasawa K, Chiba H, Fujita H, Kojima T, Saito T, Endo T, Sawada N. Possible involvement of gap junctions in the barrier function of tight junctions of brain and lung endothelial cells. J. Cell Physiol. 2006; 208:123–132. [PubMed: 16547974]

Nagy JI, Rash JE, Li X, Rempel J, Stelmack G, Patel D, Yasumura T, Staines WA. Connexin26 in adult rodent CNS: demonstration at astrocytic gap junctions and co-localization with connexin30 and connexin43. J. Comp. Neurol. 2001; 441:302–323. [PubMed: 11745652]

Nagy JI, Ionescu AV, Lynn BD, Rash JE. Coupling of astrocyte connexins Cx26, Cx30, Cx43 to oligodendrocyte Cx29, Cx32, Cx47: Implications from normal and connexin32 knockout mice. Glia. 2003a; 44:205–218. [PubMed: 14603462]

Nagy JI, Ionescu AV, Lynn BD, Rash JE. Connexin29 and connexin32 at oligodendrocyte/astrocyte gap junctions and in myelin of mouse CNS. J. Comp. Neurol. 2003b; 464:356–370. [PubMed: 12900929]

Nagy JI, Dudek FE, Rash JE. Update on connexins and gap junctions in neurons and glia in in the mammalian central nervous system. Brain Res. Rev. 2004; 47:191–215. [PubMed: 15572172]

Nagy JI, Lynn BD, Tress O, Willecke K, Rash JE. Connexin26 expression in brain parenchymal cells demonstrated by targeted connexin ablation in transgenic mice. Eur. J. Neurosci. 2011; 34:263–271. [PubMed: 21714813]

Nagy JI. Evidence for connexin36 localization at hippocampal mossy fiber terminals suggesting mixed chemical/electrical transmission by granule cells. Brain Res. 2012; 1487:107–122. [PubMed: 22771400]

Nagy JI, Bautista W, Blakley B, Rash JE. Morphologically mixed chemical-electrical synapses formed by primary afferents in rodent vestibular nuclei as revealed by immunofluorescence detection of connexin36 and vesicular glutamate transporter-1. Neuroscience. 2013; 252:468–488. [PubMed: 23912039]

Ochalski PAY, Frankenstein UN, Hertzberg EL, Nagy JI. Connexin43 in rat spinal cord: Localization in astrocytes and identification of heterotypic astro-oligodendrocytic gap junctions. Neuroscience. 1997; 76:931–945. [PubMed: 9135062]

Pastor AM, Mentis GZ, de la Cruz RR, Diaz E, Navarrete R. Increased electrotonic coupling in spinal motoneurons after transient botulinum neurotoxin paralysis in the neonatal rat. J. Neurophysiol. 2003; 89:793–805. [PubMed: 12574457]

Personius KE, Balice-Gordon RJ. Activity-dependent editing of neuromuscular synaptic connections. Brain Res. Bull. 2000; 53:513–522. [PubMed: 11165786]

Personius KE, Balice-Gordon RJ. Loss of correlated motor neuron activity during synaptic competition at developing neuromuscular synapses. Neuron. 2001; 31:395–408. [PubMed: 11516397]

Personius KE, Chang Q, Bittman K, Panzer J, Balice-Gordon RJ. Gap junctional communication among motor and other neurons shapes patterns of neural activity and synaptic connectivity during development. Cell Commun. Adhes. 2001; 8:329–333. [PubMed: 12064613]

Personius KE, Chang Q, Mentis GZ, O'Donovan MJ, Balice-Gordon RJ. Reduced gap junctional coupling leads to uncorrelated motor neuron firing and precocious neuromuscular synapse elimination. Proc. Natl. Acad. Sci. 2007; 104:11808–11813. [PubMed: 17609378]

Rash JE, Dillman RK, Bilhartz BL, Duffy HS, Whalen LR, Yasumura T. Mixed synapses discovered and mapped throughout mammalian spinal cord. Proc. Natl. Acad. Sci. 1996; 93:4235–4239. [PubMed: 8633047]

Rash JE, Yasumura T, Dudek FE. Ultrastructure, histological distribution, and freeze-fracture immunocytochemistry of gap junctions in rat brain and spinal cord. Cell Biol. Internat. 1998a; 22:731–749.

Rash JE, Yasumura T, Hudson CS, Agre P, Nielsen S. Direct immunogold labeling of aquaporin-4 in "square arrays" of astrocyte and ependymocyte plasma membranes in rat brain and spinal cord. Proc. Natl. Acad. Sci., (USA). 1998b; 95:11981–11986. [PubMed: 9751776]

Rash JE, Yasumura T. Direct immunogold labeling of connexins and aquaporin4 in freeze-fracture replicas of liver, brain and spinal cord: factors limiting quantitative analysis. Cell Tissue Res. 1999; 296:307–321. [PubMed: 10382274]

Rash JE, Staines WA, Yasumura T, Pate D, Hudson CS, Stelmack GL, Nagy J. Immunogold evidence that neuronal gap junctions in adult rat brain and spinal cord contain connexin36 (Cx36) but not Cx32 or Cx43. Proc. Natl. Acad. Sci. 2000; 97:7573–7578. [PubMed: 10861019]

Rash JE, Yasumura T, Davidson K, Furman CS, Dudek FE, Nagy JI. Identification of cells expressing Cx43, Cx30, Cx26, Cx32 and Cx36 in gap junctions of rat brain and spinal cord. Cell Commun. Adhes. 2001a; 8:315–320. [PubMed: 12064610]

Rash JE, Yasumura T, Dudek FE, Nagy JI. Cell-specific expression of connexins and evidence for restricted gap junctional coupling between glial cells and between neurons. J. Neurosci. 2001b; 21:1983–2000. [PubMed: 11245683]

Rash JE, Olson CO, Davidson KGV, Yasumura T, Kamasawa N, Nagy JI. Identification of connexin36 in gap junctions between neurons in rodent locus coeruleus. Neuroscience. 2007a; 147:938–956. [PubMed: 17601673]

Rash JE, Davidson KG, Kamasawa N, Yasumura T, Kamasawa M, Zhang C, Michaels R, Restrepo D, Ottersen OP, Olson CO, Nagy JI. Ultrastructural localization of connexins (Cx36, Cx43, Cx45), glutamate receptors and aquaporin-4 in rodent olfactory mucosa, olfactory nerve and olfactory blub. J. Neurocytol. 2005; 34:307–341. [PubMed: 16841170]

Rash JE, Olson CO, Pouliot WA, Davidson KGV, Yasumura T, Furman CS, Royer S, Kamasawa N, Nagy JI, Dudek FE. Connexin36 vs connexin32, “miniature” neuronal gap junctions, and limited electrotonic coupling in rodent suprachiasmatic nucleus. Neuroscience. 2007b; 149:350–371. [PubMed: 17904757]

Rash JE. Molecular disruptions of the panglial syncytium block potassium siphoning and axonal saltatory conduction: pertinence to neuromyelitis optica and other demyelinating diseases of the central nervous system. Neuroscience. 2010; 168:982–1008. [PubMed: 19850107]

Severs NJ, Rothery S, Dupont E, Coppen SR, Yeh HI, Ko YS, Matsushita T, Kaba R, Halliday D. Immunocytochemical analysis of connexin expression in the healthy and diseased cardiovascular system. Microsc. Res. Tech. 2001; 52:301–322. [PubMed: 11180622]

Simon AM, McWhorter AR. Vascular abnormalities in mice lacking the endothelial gap junction proteins connexin37 and connexin40. Dev. Biol. 2002; 251:206–220. [PubMed: 12435353]

Smirnova L, Grafe A, Seiler A, Schumacher S, Nitsch R, Wulczyn FG. Regulation of miRNA expression during neural cell specification. Europ. J. Neurosci. 2005; 21:1469–1477.

Söhl G, Degen J, Teubner B, Willecke K. The murine gap junction gene connexin36 is highly expressed in mouse retina and regulated during brain development. FEBS Lett. 1998; 428:27–31. [PubMed: 9645468]

Sohl G, Maxeiner S, Willecke K. Expression and functions of neuronal gap junctions. Nat. Rev. Neurosci. 2005; 6:191–200. [PubMed: 15738956]

Sprinkle TJ. 2',3'-cyclic nucleotide 3'-phosphodiesterase, an oligodendrocyte-Schwann cell and myelin-associated enzyme of the nervous system. Crit. Rev. Neurobiol. 1989; 1989:235–301. [PubMed: 2537684]

Tresch MC, Kiehn O. Motor coordination without action potentials in the mammalian spinal cord. Nature. 2000; 3:593–599.

Tresch MC, Kiehn O. Synchronization of motor neurons during locomotion in the neonatal rat: predictors and mechanisms. J Neurosci. 2002; 22:9997–10008. [PubMed: 12427857]

van der Want JJL, Gramsbergen A, Ijema-Paassen J, de Weerd H, Liem RSB. Dendro-dendritic connections between motoneurons in the rat spinal cord: an electron microscopic investigation. Brain Res. 1998; 779:342–345. [PubMed: 9473719]

Vis JC, Nicholson LF, Faull RL, Evans WH, Severs NJ, Green CR. Connexin expression in Huntington's diseased human brain. Cell Biol. Int. 1998; 22:837–847. [PubMed: 10873295]

Walton KD, Navarette R. Postnatal changes in motoneurone electronic coupling studied in the *in vitro* rat lumbar spinal cord. J. Physiol. 1991; 433:283–305. [PubMed: 1668753]

Wilson JM, Cowan AI, Brownstone RM. Heterogeneous electrotonic coupling and synchronization of rhythmic bursting activity in mouse Hb9 Interneurons. J. Neurophysiol. 2007; 98:2370–2381. [PubMed: 17715199]

Yamamoto T, Ochalski A, Hertzberg EL, Nagy JI. On the organization of astrocytic gap junctions in rat brain as demonstrated by LM and EM immunohistochemistry of connexin43 expression. J. Comp. Neurol. 1990; 302:853–883. [PubMed: 1964467]

Yates C, Garrison K, Reese NB, Charlesworth A, Garcia-Rill E. Novel mechanism for hyperreflexia and spasticity. Prog. Brain Res. 2011; 188:167–180. [PubMed: 21333809]

Yeh H-I, Rothery S, Dupont E, Coppen SR, Severs NJ. Individual gap junction plaques contain multiple connexins in arterial endothelium. Circ. Res. 1998; 83:1248–1263. [PubMed: 9851942]

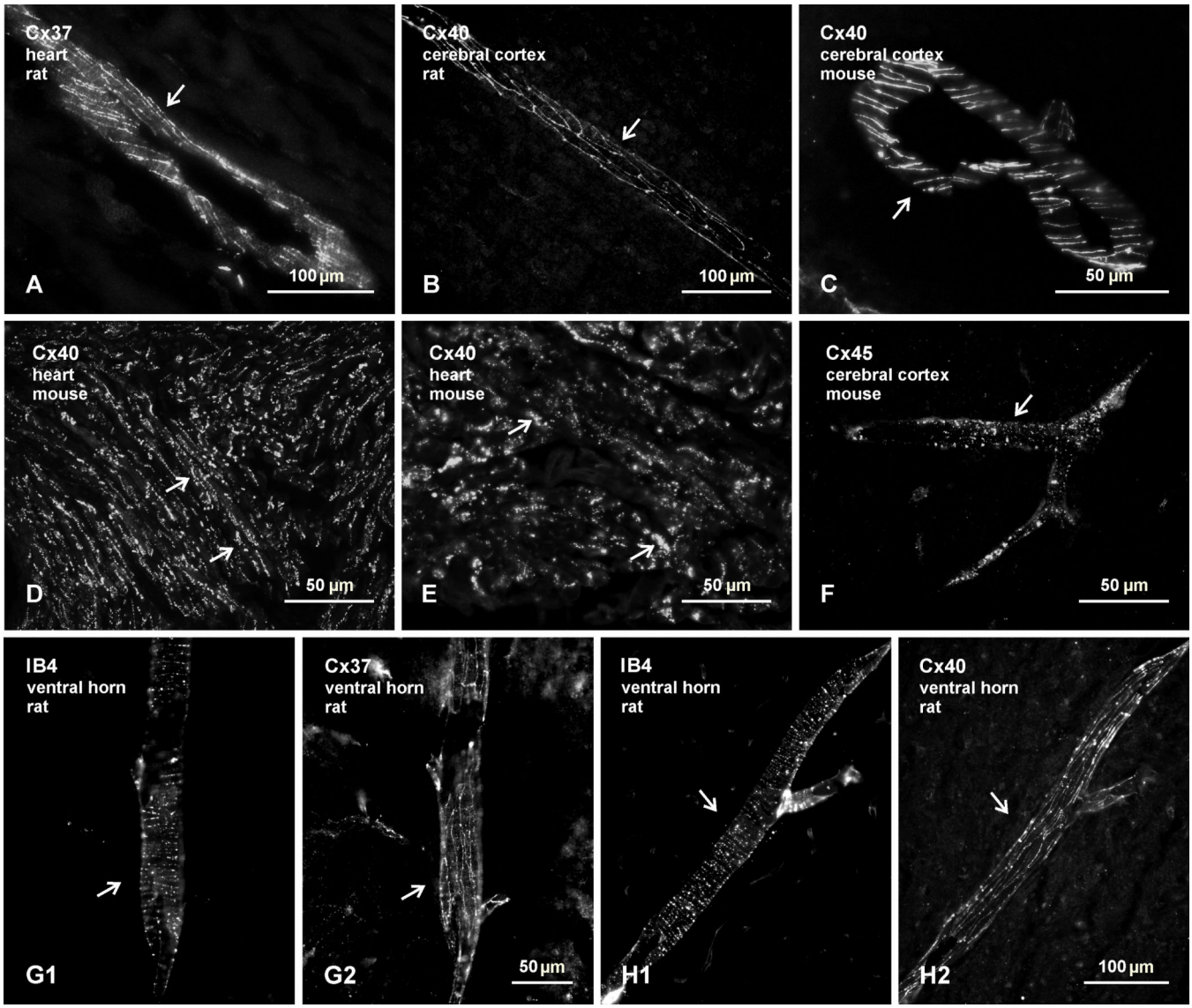

Fig. 1.

Confirmation of immunofluorescence labelling with anti-connexin antibodies in various tissues of adult rat and mouse. (A–C) Immunolabelling for Cx37 in rat heart (A), and Cx40 in rat (B) and mouse (C) cerebral cortex, showing detection of linear arrangements of these connexins along blood vessels (arrows), in accordance with patterns of their organization and localization at gap junctions between endothelial cells. (D,E) Labelling for Cx40 at low (D) and higher (E) magnification in atrium of mouse heart, where Cx40 is concentrated in gap junctions between lateral membranes of cardiomyocytes (D, arrows) and in gap junctions at intercalated discs (E, arrows). (F) Labelling of Cx45 along a blood vessel in mouse cerebral cortex (arrow), reflecting association of Cx45-puncta with vascular smooth muscle cells. (G,H) Images showing blood vessels in the spinal cord ventral horn labelled for the vessel marker IB4 (G1,H1, arrows) and images of the same vessels labelled for either Cx37 (G2, arrow) or Cx40 (H2, arrow), respectively, confirming vascular localization of the two connexins in spinal cord.

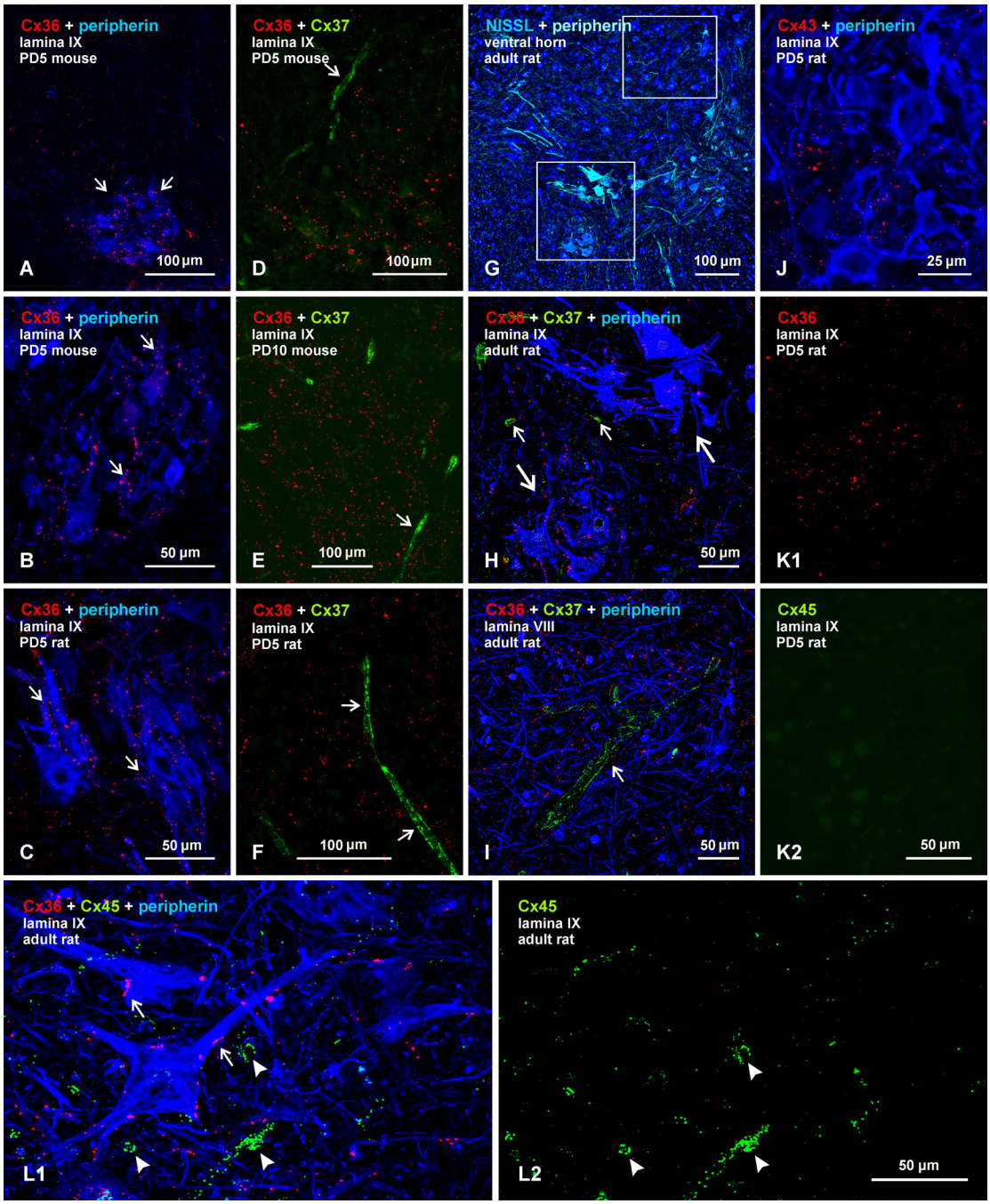

Fig. 2.

Comparison of immunofluorescence labelling for Cx36, Cx37, Cx43 and Cx45 among lumbar spinal motoneurons in lamina IX of neonatal and adult mouse and rat. In all figures, color code for secondary antibody fluorochrome and target protein is as indicated. (A–C) Images showing Cx36-puncta among peripherin-positive motoneurons (A, arrows) in mouse spinal cord at PD5, and higher magnification showing association of Cx36-puncta with motoneuron somata and dendrites in mouse (B, arrows) and rat (C, arrows) spinal cord at PD5. (D–F) Double immunofluorescence for Cx36 and Cx37 among motoneurons

(peripherin labelling excluded), showing widely distributed Cx36-puncta in mouse at PD5 (D) and PD10 (E), and in rat at PD5 (F), with labelling for Cx37 restricted to blood vessels (arrows). (G) Adult rat spinal cord ventral horn labelled for peripherin and counterstained with blue fluorescence Nissl. (H,I) Magnifications of boxed areas in G (H, lower box; I, upper box) triple labelled for Cx36, Cx37 and peripherin, showing Cx36-puncta among two peripherin-positive motoneuronal groups (H, large arrows), absence of labelling for Cx37 among these groups, and labelling of Cx37 restricted to small blood vessels (H, small arrows) and a single large vessel in lamina VIII (I, arrow). (J) Double labelling of Cx43 with peripherin in lamina IX of rat at PD5, showing very little association of sparsely-distributed Cx43-puncta with the surface of peripherin-positive motoneurons. (K) Double labelling of Cx36 with Cx45 in lamina IX of rat at PD5, showing Cx36-puncta among motoneurons (K1) and only a low level of background fluorescence in the same field labelled for Cx45 (K2). (L) Triple labelling for Cx36, Cx45 and peripherin in lamina IX of adult rat, showing Cx36-puncta on the surface of peripherin-positive motoneurons (L1, arrows), minimal Cx45 localization to these neurons, and association of Cx45 with what appear to be blood vessels (L1, arrowheads), also shown in the same field with labelling of Cx45 alone (L2).

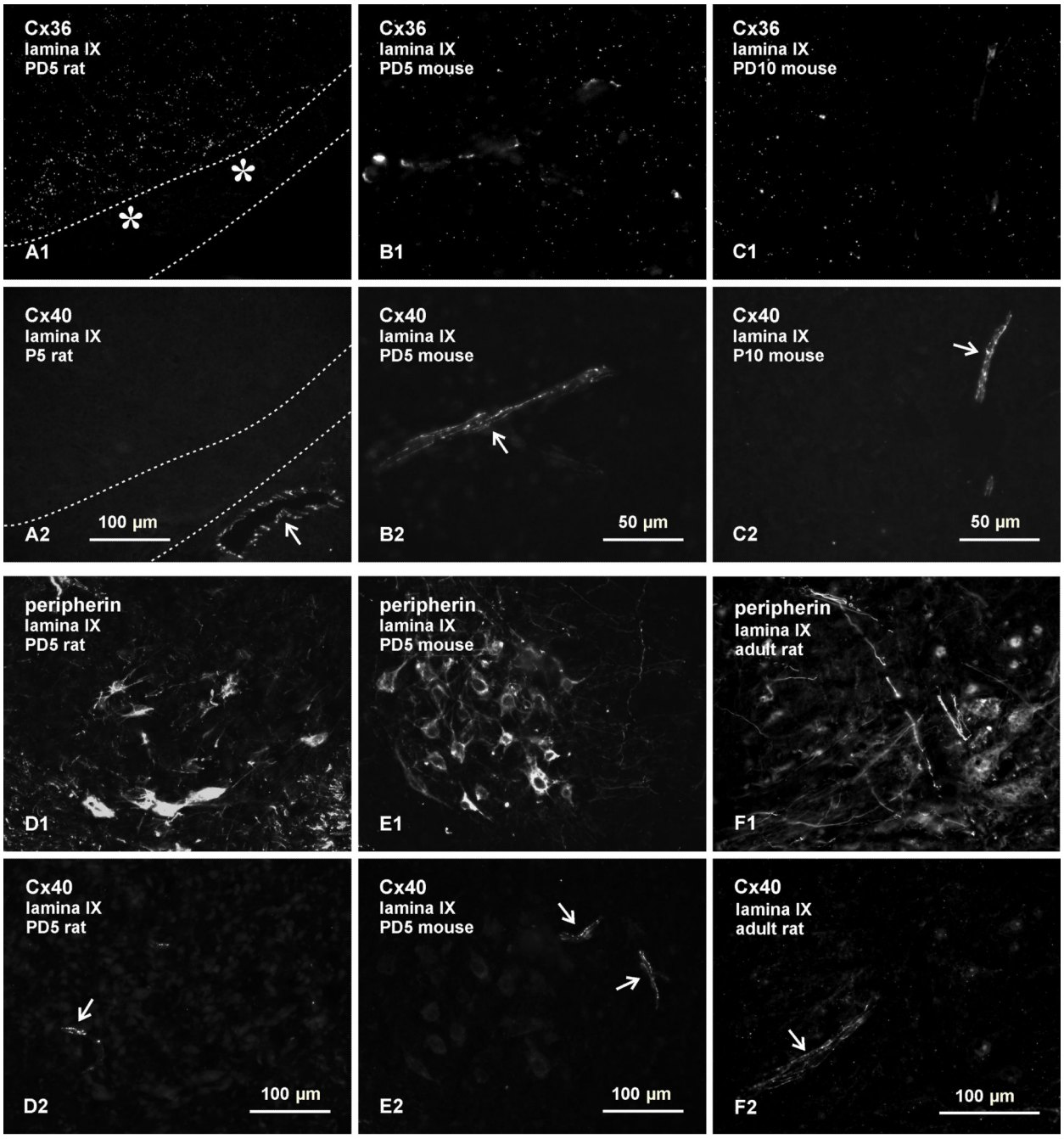

Fig. 3.

Immunofluorescence labelling for Cx36, Cx40 and peripherin in lamina IX of lumbar spinal cord in rat and mouse. Double labelling is shown in the same fields in pairs of images: A1,A2; B1,B2, etc, through to F1,F2. (A–C) Fields displaying punctate labelling for Cx36 (A1, B1 and C1) in lamina IX show labelling for Cx40 only along blood vessels in rat at PD5 (A2, arrow), and in mouse at PD5 (B2, arrow) and at PD10 (C2, arrow). The image in (A) shows a portion of ventral white matter (delineated by dotted lines) to allow inclusion of an underlying blood vessel as a positive control for labelling of Cx40. (D,E) Labelling of

peripherin (D1,E1) and Cx40 (D2,E2) in lamina IX, showing absence of labelling for Cx40 specifically within or among peripherin-positive motoneurons, and association of Cx40 with blood vessels (arrows) in rat (D) and mouse (E) at PD5. (F) Labelling of peripherin (F1) and Cx40 (F2) in lamina IX of adult rat, showing absence of labelling for Cx40 in association with peripherin-positive motoneurons, and association of Cx40 with a blood vessel (F2, arrow).

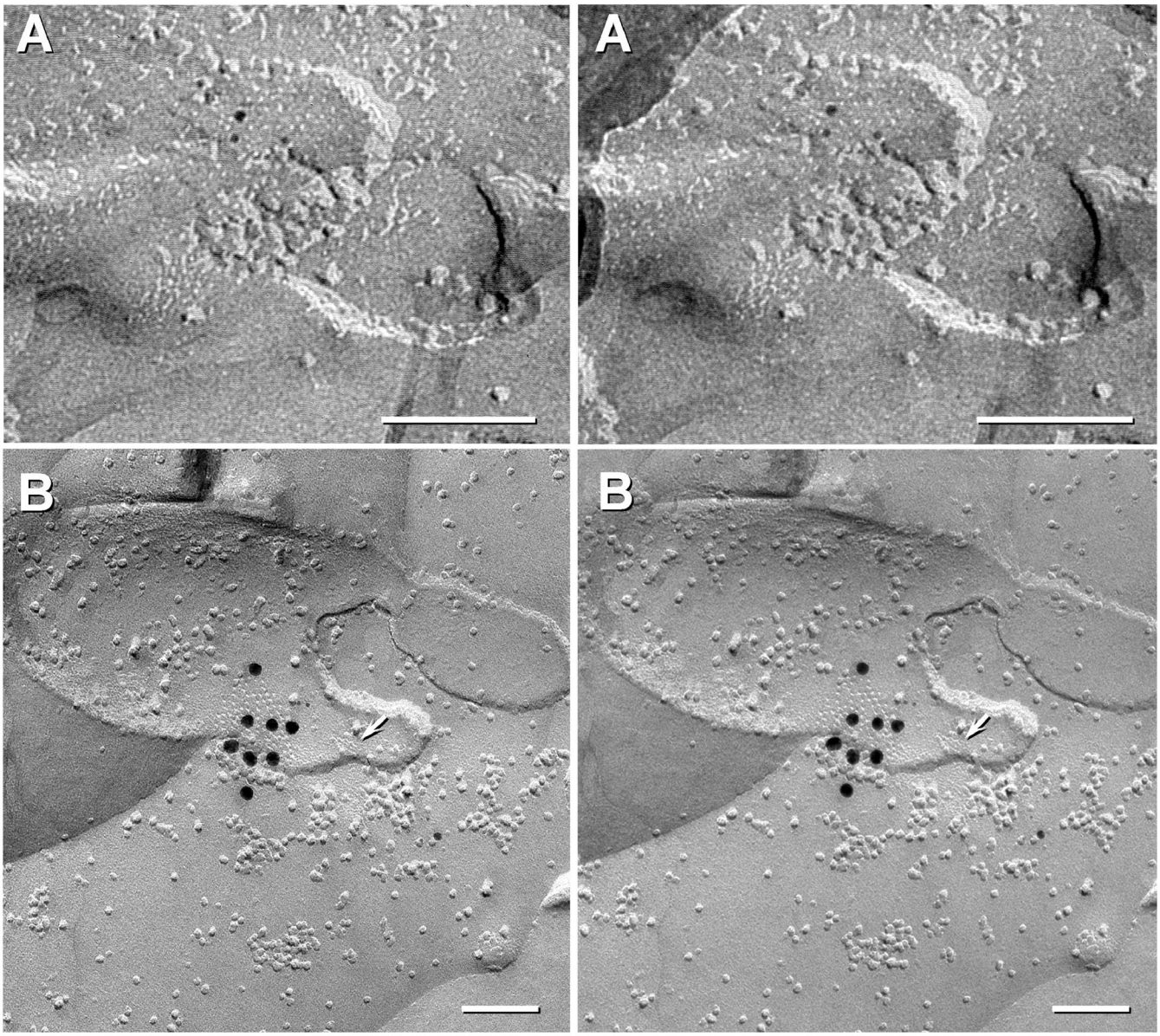

Fig. 4.

Stereoscopic FRIL images of neuronal vs. astrocyte gap junctions in developing rat spinal cord. (A) Small neuronal gap junction in P7 spinal cord labelled for Cx36 by three 5-nm gold beads but not labelled for Cx43 (10-nm and 20-nm gold; none present). (B) A medium-size astrocyte gap junction from P4 spinal cord labelled for Cx43 by eight 18 nm gold beads. This replica was also labelled for AQP4 (6 and 12nm gold beads). Arrow points to an E-face imprint of a square array, clearly marking this as an A/A gap junction. Calibration bars are 0.1 micron.

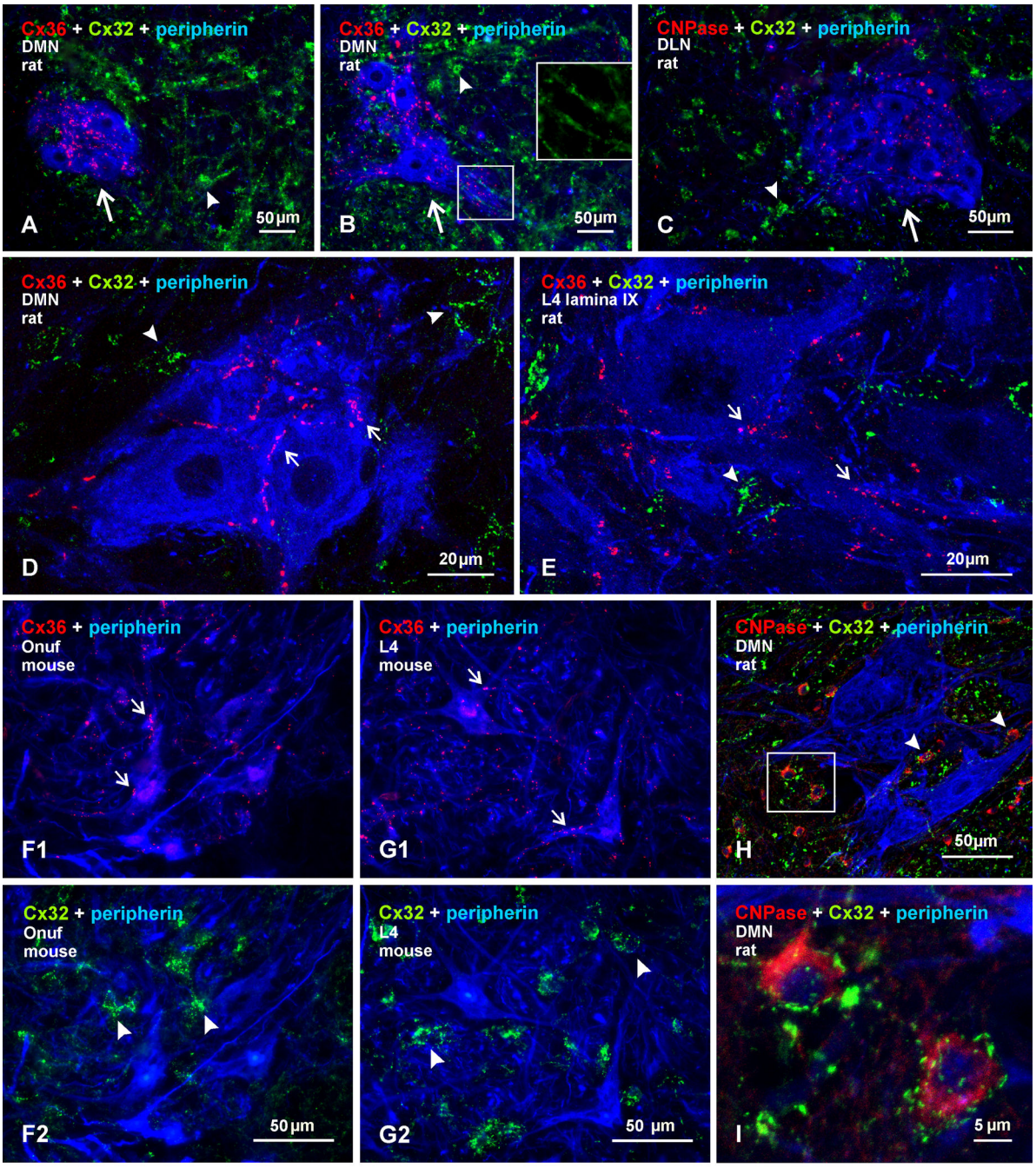

Fig. 5.

Immunofluorescence labelling for Cx36, Cx32, and peripherin in sexually dimorphic and non-dimorphic lumbar motor nuclei in adult male rat and mouse spinal cord. (A–C) Images from rat showing rostral (A) and caudal (B) regions of the dimorphic dorsomedial nucleus (DMN), and the dorsolateral nucleus (DLN), shown in (C). Cx36-puncta are seen among clusters of peripherin-positive motoneurons (arrows), and labelling for Cx32 is seen largely in surrounding regions (arrowheads). Boxed area (B, lower box; magnified in inset of upper box, without labelling for peripherin) shows Cx32 localized to myelinated fibers passing

between motoneuron dendrites. (D,E) Higher magnifications showing Cx36-puncta localized to the surface of peripherin-positive motoneurons in the dorsomedial dimorphic nucleus (D, arrows) and in a non-dimorphic motor nucleus at L4 (E, arrows), with little Cx32 (arrowheads) association at motoneurons. Cx36-puncta follow apposition of two neuronal somata (D, left arrow). (F) Images of sexually dimorphic Onuf's nucleus in mouse, showing Cx36-puncta associated with peripherin-positive Onuf motoneurons (F1, arrows) and, in the same field, labelling for Cx32 localized to small cells among these motoneurons (F2, arrowheads). (G) Image of non-dimorphic motor nucleus from L4 of mouse, showing a similar pattern of Cx36-puncta associated with motoneurons (G1, arrows), and labelling for Cx32 at small cells (G2, arrowheads). (H,I) Triple labelling for Cx32, CNPase and peripherin in the dorsomedial dimorphic nucleus at low magnification (H), with boxed area in H magnified in (I), showing Cx32 localized to CNPase-positive oligodendrocytes (arrowheads) and not to peripherin-positive motoneurons.

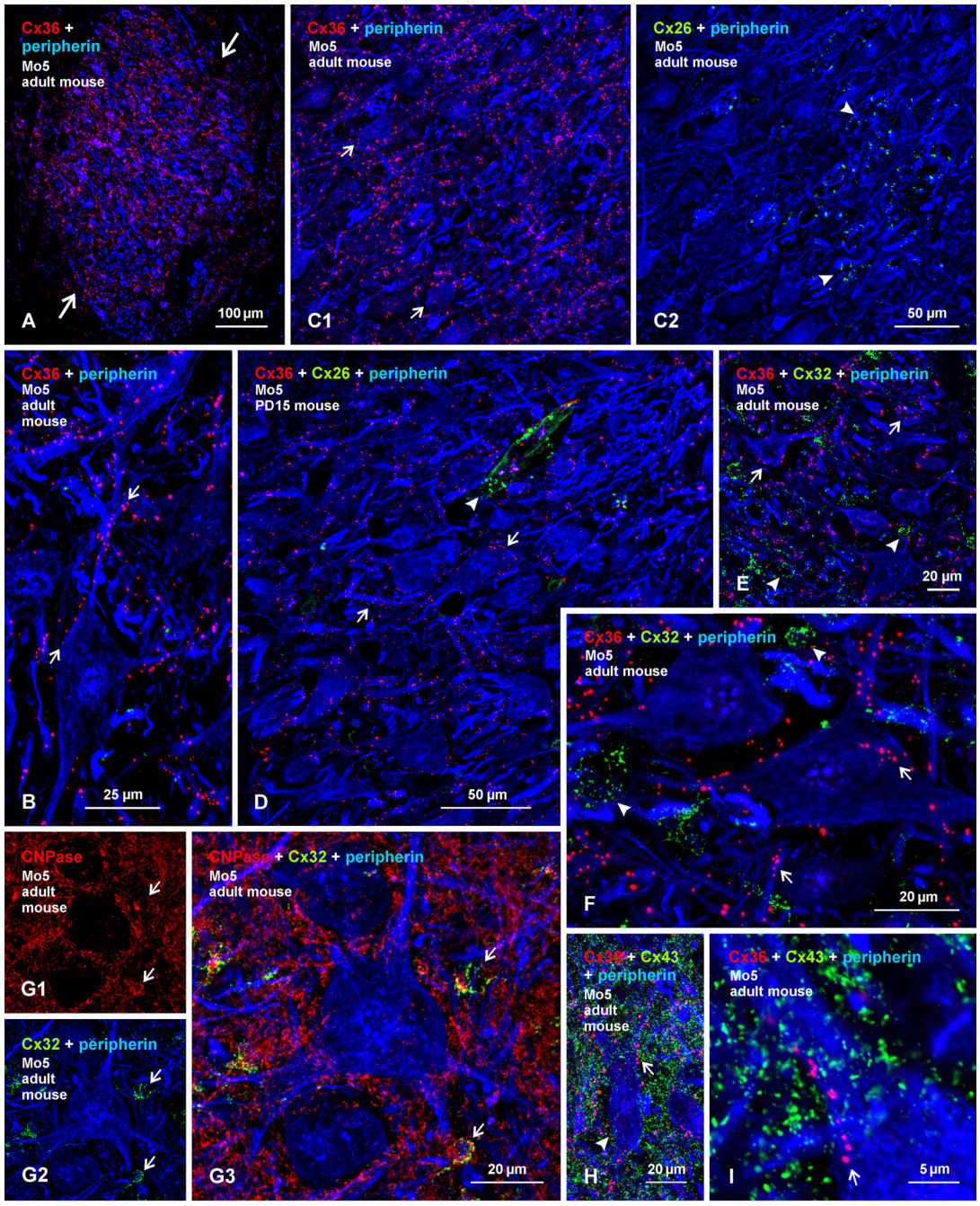

Fig. 6.

Immunofluorescence labelling of Cx36, Cx26, Cx32, Cx43, peripherin and CNPase in the trigeminal motor nucleus (Mo5) of adult and PD15 mouse. (A) Low magnification showing a high density of labelling for Cx36 among peripherin-positive motoneurons in adult mouse Mo5 (large arrows) and sparse labelling in surrounding regions. (B) Magnification showing punctate appearance of labelling for Cx36, association of Cx36-puncta with motoneuron somata and dendrites (arrows), and absence of intracellular labelling for Cx36. (C) Triple immunofluorescence showing overlay of labelling for Cx36 with peripherin and, in the same

field, overlay of labelling for Cx26 and peripherin. Cx36-puncta are seen throughout the field, including those associated with medially located motoneurons (C1, arrows), while Cx26-puncta are seen restricted to the lateral edge of the Mo5, in a region largely devoid of peripherin-positive motoneuron somata, but containing bundles of peripherin-positive myelinated fibers in the motor root of the trigeminal nerve (C2, arrowheads). (D) Triple labelling in Mo5 at PD15, showing Cx36-puncta decorating motoneuron somata and dendrites (arrows), absence Cx26 labelling in or around these somata, and Cx26-puncta associated with leptomeninges along a blood vessel (arrowhead). (E,F) Low (E) and higher (F) magnification showing labelling of Cx36 and Cx32 among peripherin-positive Mo5 motoneurons. Cx36-puncta are seen on the surface (confirmed by confocal through focus analysis) of peripherin-positive motoneurons (arrows), while Cx32-puncta are largely in regions devoid of peripherin labelling (arrowheads). (G) Triple labelling, showing CNPase localized to oligodendrocyte somata (G1, arrows) and myelinated fibers, and localization of Cx32-puncta to CNPase-positive oligodendrocyte somata (G2, arrows), as shown in overlay (G3, arrows). (H,I) Low (H) and higher (I) magnification showing overlay of triple labelling for Cx36 and Cx43 among peripherin-positive Mo5 motoneurons. Dense Cx43-puncta are seen in the vicinity of motoneurons (arrowhead), and display a random distribution compared with lining of Cx36-puncta on the surface of motoneurons (H,I, arrows). Motoneurons lack intracellular labelling for Cx43 (confirmed by confocal through focus analysis).